

Received November 5, 2018, accepted December 4, 2018, date of publication December 10, 2018, date of current version January 4, 2019.

Digital Object Identifier 10.1109/ACCESS.2018.2885784

Research on the Active Guidance Control System in High Speed Maglev Train

MINGDA ZHAI¹, AMING HAO, XIAOLONG LI, AND ZHIQIANG LONG

National University of Defense Technology, Changsha 410073, China

Corresponding author: Zhiqiang Long (lzq@maglev.cn)

This work was supported by the National Key R&D Program of China under Grant 2016YFB1200602.

ABSTRACT The guidance system is one of the important subsystems of high-speed maglev train. The active guidance of high-speed maglev train is achieved by the attraction between the guide way and the electromagnets mounted on the side of the carriage. The working characteristics of the guidance system vary according to the different guide ways and weather conditions. In the straight line, the guiding current is very small. When suffering from the bend or big crosswind, the guiding current will be very large. Therefore, the model of the guidance system has greater uncertainty, and the guidance controller is more difficult to design. This paper presents a method to make the high-speed maglev train to obtain a stable guidance ability in different conditions. The mathematical model of the guidance system is established, and the robust guidance controller is designed by H_∞ control theory. The simulation and experiment demonstrate that the high-speed maglev train using the designed guidance controller has relatively desirable performance and achieves stable guidance ability successfully.

INDEX TERMS High-speed maglev train, guidance system, nonlinear control system, robust control, H_∞ .

I. INTRODUCTION

Compared with conventional high-speed railway system, the high-speed maglev train takes full advantage of electromagnetic force to achieve active levitation and guidance and drives the train by the linear motor [1]–[3]. It completely abandons the wheel-rail relationship and the catenary-pantograph relationship for the sake of non friction. Therefore, the running speed of high-speed maglev train is easily up to 500 km/h [4]. The high speed of superconducting maglev train of Japan is 603 km/h and the electromagnetic maglev train of Germany is 505 km/h [5]. In order to further increase the running speed of high-speed railway system, the high-speed maglev train begins to attract considerably increasing attention and become an active traffic field. Consequently, National Key R & D Program of China “maglev traffic system key technology” is officially carried out to solve fundamental technical problems.

The guidance system is one of the important subsystems of high-speed maglev train [6]. As shown in Fig. 1, the left and right guidance electromagnets are connected by the suspension frame, and the lateral forces produced by the guidance electromagnet are mainly transmitted by suspension frame [7]. There is only attraction between the guidance electromagnets and the guide way. The value of this attraction changes with the guidance current and guidance gap, but the

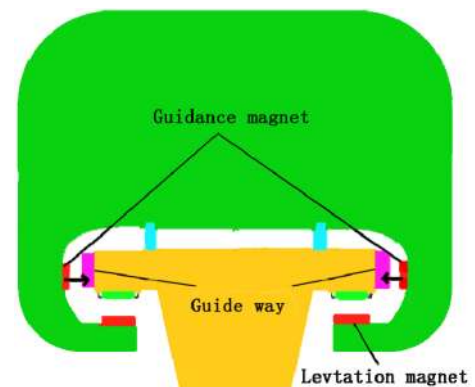


FIGURE 1. The illustration of high-speed maglev train.

direction of this attraction is unidirectional. The direction of attraction between the left guidance electromagnets and the guide way is towards right, while the direction of attraction between the right guidance electromagnets and the guide way is towards left. Guidance controllers adjust the value of the left and right attraction respectively, to ensure that the whole suspension frame is able to locate directly above the guide way centerline and doesn't move left or right.

However, the guidance system maybe suffers from different guide ways and weather conditions, the working

characteristics of the guidance system will be changed [8], [9]. Therefore, the model of the guidance system has greater uncertainty, and the guidance controller is more difficult to design

This study is conducted to make the high-speed maglev train obtain a stable guidance ability on different conditions. The mathematical model of the guidance system is established, and the robust guidance controller is designed by H_∞ control theory, which ensure the safety and improve the reliability of high-speed maglev train.

II. MATHEMATICAL MODEL OF GUIDANCE SYSTEM

In order to facilitate the modeling, the movement of the left and right directions are only considered, while the yaw and roll of the guidance electromagnet are ignored. The stiffness of guidance electromagnet is very high and the deformation is neglected. Therefore, the equivalent action-point of guidance force is in the center of mass. The suspension beam, corbel, and suspension device are equivalent to spring damping systems.

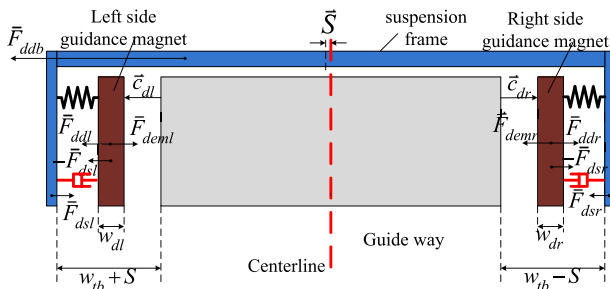


FIGURE 2. The model of guidance system in high-speed maglev train.

As shown in Fig. 2, the left guidance gap is \bar{c}_{dl} , and the right guidance gap is \bar{c}_{dr} . The external interference force on the left guidance electromagnet is \bar{F}_{ddb} , and the right guidance electromagnet is \bar{F}_{ddr} . The mass of left guidance electromagnet is m_{dl} , and the width is w_{dl} while the mass of right guidance electromagnet is m_{dr} , and the width is w_{dr} . The natural length, stiffness and damping of equivalent spring damper system connected to left guidance electromagnet are l_{dl0} , k_{dl} , and η_{dl} respectively, and the right are l_{dr0} , k_{dr} and η_{dr} . The voltage and current of left guidance electromagnet is u_{dcl} and i_{dl} ; the electromagnetic force is \bar{F}_{deml} and the restoring force acting on suspension frame by spring damper system is \bar{F}_{dsl} . The voltage and current of right guidance electromagnet are u_{dcr} and i_{dr} ; the electromagnetic force is \bar{F}_{demr} , and the restoring force acting on suspension frame by spring damper system is \bar{F}_{dsr} . The equivalent mass of suspension frame is m_{db} and the interference force is \bar{F}_{ddb} ; The gap between the inside of suspension frame and guide way is $2w_{ib}$, and the displacement of suspension frame away from central line is \bar{S} .

The number of turns, the resistance, the polar area and the permeability of vacuum are N_d , R_d , A_d and μ_0 respectively. Thus, the equations of guidance system are obtained

as follows:

$$u_{dcl}(t) = R_d i_{dl}(t) + \frac{d}{dt} \left(\frac{N_d^2 i_{dl}(t)}{2c_{dl}(t)/\mu_0 A_d} \right)$$

$$u_{dcr}(t) = R_d i_{dr}(t) + \frac{d}{dt} \left(\frac{N_d^2 i_{dr}(t)}{2c_{dr}(t)/\mu_0 A_d} \right)$$

$$F_{deml}(i_{dl}, c_{dl}) = \frac{\mu_0 N_d^2 A_d}{4} \left[\frac{i_{dl}}{c_{dl}} \right]^2$$

$$F_{demr}(i_{dr}, c_{dr}) = \frac{\mu_0 N_d^2 A_d}{4} \left[\frac{i_{dr}}{c_{dr}} \right]^2$$

$$F_{dsl} = k_{dl}[(w_{ib} + S - c_{dl} - w_{dl}) - l_{dl0}] - \eta_{dl}[\dot{c}_{dl}(t) - \dot{S}(t)]$$

$$F_{dsr} = k_{dr}[(w_{ib} - S - c_{dr} - w_{dr}) - l_{dr0}] - \eta_{dr}[\dot{c}_{dr}(t) + \dot{S}(t)]$$

$$m_{dl} \ddot{c}_{dl} = F_{dsl} + F_{ddl} - F_{deml}$$

$$m_{dr} \ddot{c}_{dr} = F_{dsr} + F_{ddr} - F_{demr}$$

$$m_{db} \ddot{S} = F_{ddb} - F_{dsl} + F_{dsr}$$

In the practical guidance system, the lateral stiffness of the guidance system is so large that it is regarded as a rigid body, namely, $k_{dl} = k_{dr} = \infty$, $\eta_{dl} = \eta_{dr} = 0$. Moreover, the effect of irregularity and gap measurement errors on guidance system are ignored, and the following relations are valid:

$$\Delta c_{dl} = \Delta S = -\Delta c_{dr}$$

$$\dot{c}_{dl} = \dot{S} = -\dot{c}_{dr}$$

$$\ddot{c}_{dl} = \ddot{S} = -\ddot{c}_{dr}$$

The mathematical model of guidance system is simplified, and the linearization of the above equations is done near the equilibrium point:

$$\Delta u_{dcl}(t) = R_d \Delta i_{dl}(t) + L_{dl0} \Delta \dot{i}_{dl}(t)$$

$$\Delta u_{dcr}(t) = R_d \Delta i_{dr}(t) + L_{dr0} \Delta \dot{i}_{dr}(t)$$

$$\Delta F_{deml} = k_{dil} \Delta i_{dl}(t) - k_{dzl} \Delta c_{dl}(t)$$

$$\Delta F_{demr} = k_{dir} \Delta i_{dr}(t) + k_{dzt} \Delta c_{dl}(t)$$

$$\ddot{c}_{dl}(t) = \frac{\Delta F_{emr} - \Delta F_{eml} + \Delta F_{ddl} - \Delta F_{ddr} + \Delta F_{ddb}}{(m_{dl} + m_{dr} + m_{db})}$$

Among:

$$k_{dil} = \frac{\mu_0 N_d^2 A_d i_{dl0}}{2c_{dl0}^2} k_{dir} = \frac{\mu_0 N_d^2 A_d i_{dr0}}{2c_{dr0}^2}$$

$$k_{dzl} = \frac{\mu_0 N_d^2 A_d i_{dl0}^2}{2c_{dl0}^3} k_{dzt} = \frac{\mu_0 N_d^2 A_d i_{dr0}^2}{2c_{dr0}^3}$$

$$L_{dl0} = \frac{\mu_0 N_d^2 A_d}{2c_{dl0}} L_{dr0} = \frac{\mu_0 N_d^2 A_d}{2c_{dr0}}$$

$$\begin{aligned}
 \mathbf{x} &= (x_1 \quad x_2 \quad x_3 \quad x_4)^T = (c_{dl} \quad \dot{c}_{dl} \quad i_{dl} \quad i_{dr})^T \\
 \dot{\mathbf{x}} &= \begin{pmatrix} 0 & 1 & 0 & 0 \\ \frac{\mu_0 N_d^2 A_d i_{dl0}^2 + i_{dr0}^2}{2M_d} & 0 & -\frac{\mu_0 N_d^2 A_d i_{dl0}}{2M_d} & \frac{\mu_0 N_d^2 A_d i_{dr0}}{2M_d} \\ 0 & 0 & -\frac{2R_d c_{dl0}}{\mu_0 N_d^2 A_d} & 0 \\ 0 & 0 & 0 & -\frac{2R_d c_{dl0}}{\mu_0 N_d^2 A_d} \end{pmatrix} \mathbf{x} \\
 &+ \begin{pmatrix} 0 & 0 \\ \frac{2c_{dl0}}{\mu_0 N_d^2 A_d} & 0 \\ 0 & \frac{2c_{dl0}}{\mu_0 N_d^2 A_d} \end{pmatrix} \mathbf{u} \\
 \mathbf{y} &= \begin{pmatrix} 1 & 0 & 0 & 0 \end{pmatrix} \mathbf{x} \\
 \mathbf{u} &= (u_{dcl} \quad u_{dcr})
 \end{aligned} \tag{1}$$

For conciseness, Δc_{dl} is expressed in c_{dl} the following sections, and all the other state variables are likewise. Thus, the state variables are specified, and the state space equation is become, (1), shown at the top of this page.

Where, $M_d = m_{db} + m_{dl} + m_{dr}$.

Equation (1) is shown that the model of the guidance system is uncertain, and it markedly depends on the variations of c_{dl0} , c_{dr0} , i_{dl0} and i_{dr0} . The system matrix A and the control matrix B vary according to the different working points. If the guidance electromagnet is impacted by external disturbance force during the operation, the working points of the guidance system will change consequently. Therefore, the system matrix A and the control matrix B is changed, and the model of guidance system is changed.

In the above modeling and analysis, a default situation is that the guiding current will not be zero. In fact, if the external disturbance force increases to a certain extent, the current of one electromagnet is bound to decrease down to zero and will not continue to decrease. In that case, the default situation is no longer valid, and the structure of model will also change. Without loss of generality, it is assumed that the right guiding current is reduced to zero, and the left electromagnet work normally.

Under this circumstance:

$$\begin{aligned}
 i_{dr} &= 0 \\
 k_{dir} &= \frac{\mu_0 N_d^2 A_d i_{dr0}}{2c_{dr0}^2} = 0 \\
 k_{diz} &= \frac{\mu_0 N_d^2 A_d i_{dr0}^2}{2c_{dr0}^3} = 0 \\
 \mathbf{u} &= u_{dcl}
 \end{aligned}$$

Thus, the state variables are specified:

$$\mathbf{x} = (x_1 \quad x_2 \quad x_3)^T = (c_{dl} \quad \dot{c}_{dl} \quad i_{dl})^T$$

The model of guidance system is become under this circumstance:

$$\begin{aligned}
 \dot{\mathbf{x}} &= \begin{pmatrix} 0 & 1 & 0 \\ \frac{\mu_0 N_d^2 A_d i_{dl0}^2}{2M_d} & 0 & -\frac{\mu_0 N_d^2 A_d i_{dl0}}{2M_d} \\ 0 & 0 & -\frac{2R_d c_{dl0}}{\mu_0 N_d^2 A_d} \end{pmatrix} \mathbf{x} \\
 &+ \begin{pmatrix} 0 \\ 0 \\ \frac{2c_{dl0}}{\mu_0 N_d^2 A_d} \end{pmatrix} u_{dcl} \\
 \mathbf{y} &= \begin{pmatrix} 1 & 0 & 0 \end{pmatrix} \mathbf{x}
 \end{aligned} \tag{2}$$

Consequently, the guidance system has two kinds of working model, namely, double electromagnet model and single electromagnet model. Under typical circumstance, the guidance system works in double electromagnet model. However, when the guiding current of one electromagnet decreases down to zero in order to supply adequate guidance force, the guidance system will enter in single electromagnet model.

III. ANALYSIS AND DESIGN OF GUIDANCE CONTROLLER

A. DOUBLE ELECTROMAGNET MODEL

When the guidance system is in the double electromagnet model, the two sides of electromagnets will work normally. The guidance forces are generated by guidance electromagnets to keep the guidance system in the set gap. Meanwhile, it is obvious that the guidance system is unstable but fully controllable. Therefore, the control law is able to be designed by full state feedback.

The guidance electromagnet is a typical inertia link, and the current response is seriously lagged behind the voltage change. The response time is not able to meet the demand

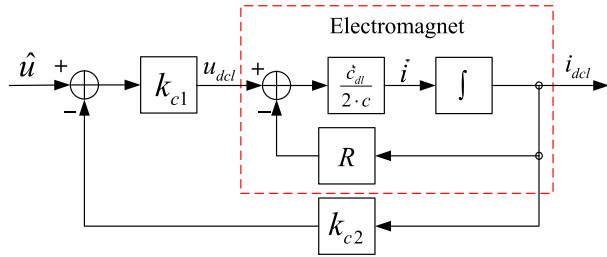


FIGURE 3. The illustration of current loop feedback.

of high-speed maglev train. Therefore, the current feedback method is adopted to reduce the response time. The schematic diagram of current loop feedback is illustrated in Fig. 3.

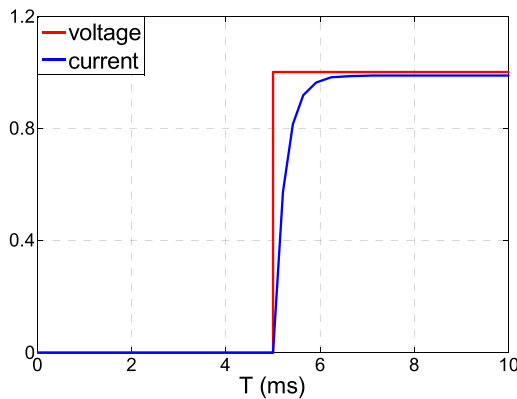


FIGURE 4. The response of electromagnet using current loop feedback.

As shown in Fig. 4, The proper selections of parameters k_{c1} and k_{c2} reduce the response time of guidance electromagnet down to 10 milliseconds. The relationship between the voltage and the current of the electromagnet is considered to be a proportional link in the frequency band of guidance system. What's more, the current feedback also decreases the order of guidance system from 4 order to 2 order.

Thus, the state variables are specified again after using the current loop feedback:

$$\mathbf{x} = (x_1 \quad x_2)^T = (c_{dl} \quad \dot{c}_{dl})^T$$

The parameters of the guidance system are indicated in above Table. 1. These parameters are brought into the model of guidance system, and the state space equation of the guidance system is become:

$$\begin{cases} \dot{\mathbf{x}} = \begin{pmatrix} 0 & 1 \\ 0.8636(i_{dl0}^2 + i_{dr0}^2) & 0 \end{pmatrix} \mathbf{x} \\ + \begin{pmatrix} 0 & 0 \\ -0.0095i_{dl0} & 0.0095i_{dr0} \end{pmatrix} \mathbf{u} \\ \mathbf{y} = \begin{pmatrix} 1 & 0 \end{pmatrix} \mathbf{x} \end{cases}$$

The method of quadratic optimal control is introduced to design a full-state feedback controller. The control goal is to keep the guidance system in the set gap. When the guidance

TABLE 1. Parameter list of guidance system.

Symbol	Meaning	Quantity	Unit
m_{dl}	Mass of left guidance electromagnet	390	kg
m_{dr}	Mass of right guidance electromagnet	390	kg
m_{db}	Equivalent mass of suspension frame	550	kg
\bar{c}_{dl}	Left guidance gap		mm
\bar{c}_{dr}	Right guidance gap		mm
i_{dl}	Left guidance current		A
i_{dr}	Right guidance current		A
u_{dcl}	Left guidance voltage		V
u_{dcr}	Left guidance voltage		V
R_d	Resistance	2.77	Ω
N_d	Number of turns	210	
μ_0	vacuum permeability	$4\pi \times 10^{-7}$	
c_{d0}	set gap	11	mm

system has no external lateral interference force in the double electromagnet model, the guiding currents will be zero under normal circumstances. However, the guiding current is not set to zero in the practical engineering. The guiding current of non disturbance is set as 5 amperes, namely, $i_{dl0} = i_{dr0} = 5A$. It's an attempt to prevent a dead zone and obtain a definite stiffness at the static working point.

The feedback parameters of controller are obtained:

$$K = \begin{pmatrix} -5461 & -723 \\ 5461 & 723 \end{pmatrix}$$

In order to overcome the impact of track irregularity and sensor measurement error, the differential control strategy is adopted in the practical controller. The differences between the left and right guiding gaps are used as feedback variables. The left and right guiding gaps are equal as control targets. Thus, the state variables are replaced:

$$\begin{cases} c_{dl} \leftarrow \frac{c_{dl} - c_{dr}}{2} \\ c_{dr} \leftarrow \frac{c_{dr} - c_{dl}}{2} \end{cases}$$

Therefore, the control law is finally represented as:

$$\mathbf{u} = \begin{pmatrix} u_{dcl} \\ u_{dcr} \end{pmatrix} = \begin{pmatrix} -5461 \frac{c_{dl} - c_{dr}}{2} - 723 \dot{c}_{dl} \\ -5461 \frac{c_{dr} - c_{dl}}{2} - 723 \dot{c}_{dr} \end{pmatrix} \quad (3)$$

If the guidance system suffers from a left external disturbance force in the double electromagnet model, the designed state feedback controller will adjust rapidly in order to keep the guidance system in set gap. The controller output increment is become: $u_{dcl} = -u_{dcr} = \Delta u_0$, and $\Delta u_0 < u_{dcr0}$ (the right guidance controller output with non disturbance). At this moment, the left and right guiding current will become

$i_{dl0} + \Delta i_{d0}$ and $i_{dr0} - \Delta i_{d0}$ ($\Delta i_{d0} < i_{dl0}$). Under this circumstance, the guidance system will deviate from the original working point and enter a new steady-state working point. The state space equation is become:

$$\begin{cases} \dot{\mathbf{x}} = \begin{pmatrix} 0 & 1 \\ 0.8636(i_{dl0}^2 + i_{dr0}^2 + 2\Delta i_{d0}^2) & 0 \end{pmatrix} \mathbf{x} \\ + \begin{pmatrix} 0 \\ -0.0095(i_{dl0} + i_{dr0}) \end{pmatrix} u_{dcr} \\ \mathbf{y} = \begin{pmatrix} 1 & 0 \end{pmatrix} \mathbf{x} \end{cases} \quad (4)$$

According to the (4), an important characteristic of guidance system is obtained in the double electromagnet model: the input matrix \mathbf{B} of the system is only related to i_{dl0} and i_{dr0} , and it will not change with the working point. It does mean that the input characteristic of the system is invariable.

In order to get an evaluation of the designed controller, the left guidance electromagnet is assumed to be impacted on a step interference force of 200 N to ensure that the guidance system will not enter the single electromagnet model. The response of guidance system in double electromagnet model is shown in Fig. 5(a) and Fig. 5(b) respectively.

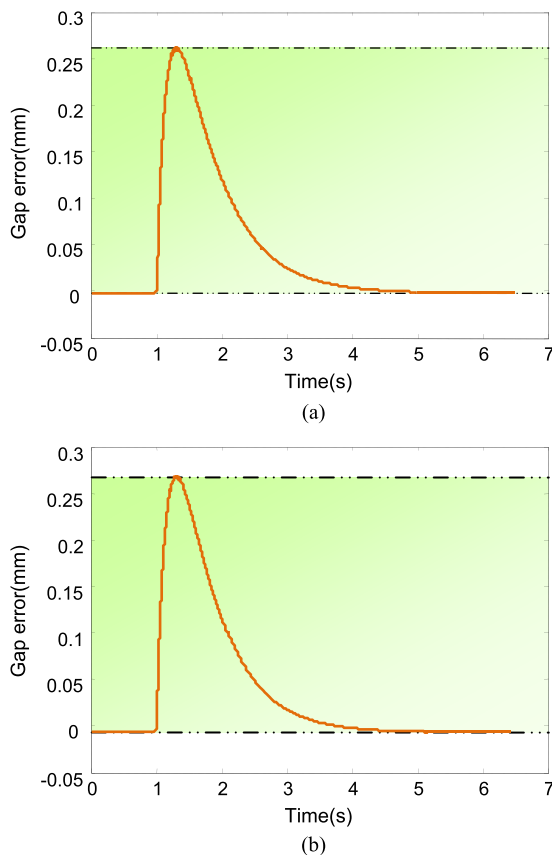


FIGURE 5. The response of guidance system with different Initial static current in double electromagnet model. (a) $i_{dl0} = i_{dr0} = 5A$. (b) $i_{dl0} = i_{dr0} = 7.5A$.

The simulation shows that the response of guidance system with different initial static current in double electromagnet

model is very analogical. A conclusion is obtained preliminarily that the guidance system serves the similar properties in double electromagnet model. If the value of i_{dl0} and i_{dr0} are set very large, the guidance system will always be in the double electromagnet model. The designed controller is completely able to meet the requirements of guidance system, and the robust controller is not needed.

However, the method of increasing the initial static current i_{dl0} and i_{dr0} is not acceptable in practical engineering. The guidance electromagnet with high current for a long time will generate a large amount of heat, which not only wastes energy, but also damages the life of electromagnet. In addition, the huge electromagnetic force generated by electromagnets on both sides will reduce the lifetime of the mechanical structures of guidance system and increase the failure rate [10], [11]. Most important of all, the large guidance force at the initial working point is useless and doesn't supply guidance ability.

Based on the above analysis, the initial static current of non disturbance is better to be set as 5A, namely, $i_{dl0} = i_{dr0} = 5A$. A new situation will occur that the guidance system will enter single electromagnet model easily when the guidance system suffers from a small external disturbance force.

B. SINGLE ELECTROMAGNET MODEL

When the guidance system is in the single electromagnet model, only one electromagnets will work normally. The guidance forces are generated by one guidance electromagnet to keep the guidance system in the set gap.

If the guidance system suffers from a left external disturbance force in the single electromagnet model, the designed state feedback controller will adjust rapidly in order to go back to the equilibrium position. The controller output increment is become: $u_{dcl} = -u_{dcr} = \Delta u'_0$, and $\Delta u'_0 > u_{dcr0}$. Since the power device of guidance controller adopts the half bridge structure, the right guiding current will become zero and the left guiding current will become $i_{dl0} + \Delta i'_{d0}$. In other words, the guidance system is working in the single electromagnet model at this moment. The system state space equation is accordingly become:

$$\begin{cases} \dot{\mathbf{x}} = \begin{pmatrix} 0 & 1 \\ 0.8636(i_{dl0} + \Delta i_{d0})^2 & 0 \end{pmatrix} \mathbf{x} \\ + \begin{pmatrix} 0 \\ -0.0095(i_{dl0} + \Delta i_{d0}) \end{pmatrix} u_{dcr} \\ \mathbf{y} = \begin{pmatrix} 1 & 0 \end{pmatrix} \mathbf{x} \end{cases} \quad (5)$$

It is determined that the input characteristic of the guidance system in single electromagnet model loses invariability, and the input matrix \mathbf{B} changes with Δi_{d0} .

When the guidance system transits from double electromagnet mode to single electromagnet mode, the system model has changed. It should be particular noted that the system characteristics have not changed abruptly. Therefore, the designed controller is still applicable.

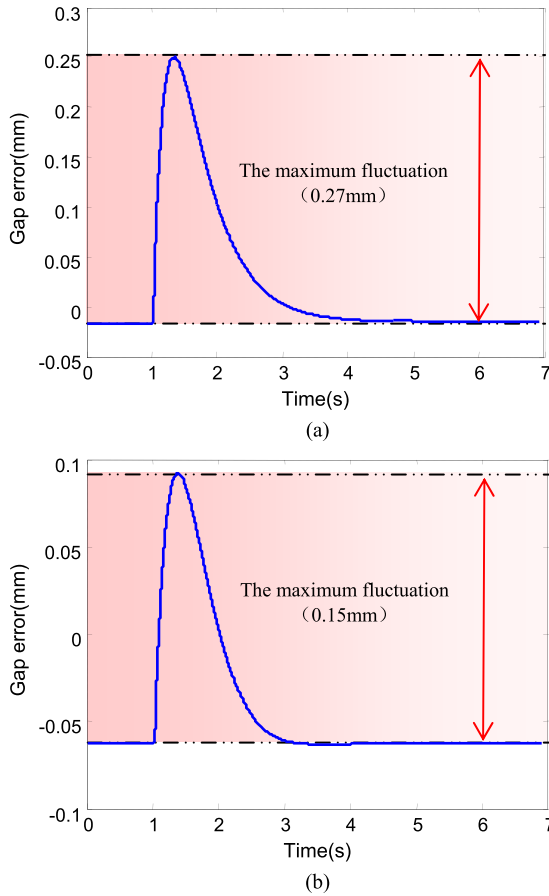


FIGURE 6. The response of guidance system with different Initial static current in single electromagnet model. (a) $i_{dl0} = 10A$. (b) $i_{dl0} = 20A$.

In order to have an evaluation of the designed controller in the single electromagnet model, the left guidance electromagnet is assumed to be impacted on a step interference force of 200 N. The response of guidance system in single electromagnet model are shown in Fig. 6(a) and Fig. 6(b) respectively.

When the initial static working current of left guidance electromagnet is set as 10 A, the maximum gap error fluctuation is 0.27 mm. When the initial static working current is set as 20 A, the maximum gap error fluctuation becomes 0.15 mm. What's more, the initial static working current is larger so that the initial gap error is far away from zero. The simulation results demonstrate that the properties of guidance system in single electromagnet model are significantly different with different initial static working current, and the robust controller is needed to be designed.

IV. DESIGN FOR ROBUST GUIDANCE CONTROLLER

As mentioned above analysis, the uncertainty of guidance system is mainly caused by the relatively great change of the static working current. When the guidance system is in the single electromagnet model, the state space equation

of guidance system is represented with consideration of the uncertainty of the static working current.

$$\begin{cases} \dot{\mathbf{x}} = \begin{pmatrix} 0 & 1 & 0 \\ \frac{\mu_0 N_d^2 A_d}{2M_d c_{dl0}^3} (i_{dl0} + \Delta i_{dl0})^2 & 0 & -\frac{\mu_0 N_d^2 A_d}{2M_d c_{dl0}^2} (i_{dl0} + \Delta i_{dl0}) \\ 0 & 0 & -\frac{R_d}{L_{dl0}} \end{pmatrix} \mathbf{x} \\ + \begin{pmatrix} 0 \\ 0 \\ 1 \\ \frac{1}{L_{dl0}} \end{pmatrix} u_{dcl} \\ \mathbf{y} = \begin{pmatrix} 1 & 0 & 0 \end{pmatrix} \mathbf{x} \end{cases} \quad (6)$$

In practical engineering, the biggest change of working current of the guidance system is almost no more than 50%. It is assumed that the static working current of guidance system varies in the range of $\pm 50\%$. The disturbance δ_{i0} is introduced and belongs to $[-1, 1]$. Therefore, $i_{dl0} + \Delta i_{dl0}$ is written as $i_{dl0}(1 + 0.5\delta_{i0})$. Equation (6) is reformulated as:

$$\begin{cases} \dot{\mathbf{x}} = \begin{pmatrix} 0 & 1 & 0 \\ \frac{k_{dzl0}}{M_d} (1 + \delta_{i0} + 0.25\delta_{i0}^2) & 0 & -\frac{k_{dil0}}{M_d} (1 + 0.5\delta_{i0}) \\ 0 & 0 & -\frac{R_d}{L_{dl0}} \end{pmatrix} \mathbf{x} \\ + \begin{pmatrix} 0 \\ 0 \\ 1 \\ \frac{1}{L_{dl0}} \end{pmatrix} u_{dcl} \\ \mathbf{y} = \begin{pmatrix} 1 & 0 & 0 \end{pmatrix} \mathbf{x} \end{cases} \quad (7)$$

where $k_{dzl0} = 0.8636i_{dl0}^2$, $k_{dil0} = -0.0095i_{dl0}$

According to (7), the structure of guidance control system considering disturbance is achieved in Fig. 7.

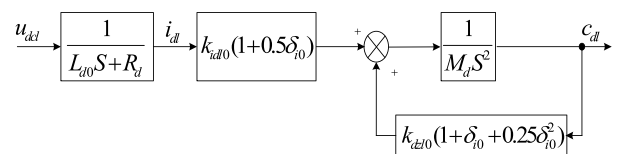


FIGURE 7. The structure of guidance control system considering disturbance.

In order to obtain the standard form of a robust control system, the disturbance term $k_{dil0}(1 + 0.5\delta_{i0})$ is expressed as the multiplicative uncertainties; the disturbance term $k_{dzl0}(1 + \delta_{i0} + 0.25\delta_{i0}^2)$, which contains a square term, is difficult to correspond to the common uncertainty directly. Therefore, the linear fractional transformation (LFT) is

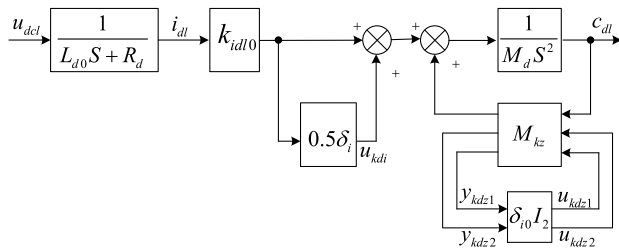


FIGURE 8. The transformed structure of guidance control system.

adopted for disturbance separation [12]. The disturbance term $k_{dzl0}(1 + \delta_{i0} + 0.25\delta_{i0}^2)$ is transformed:

$$k_{dzl0}(1 + \delta_{i0} + 0.25\delta_{i0}^2) = F_l(\mathbf{M}_{kz}, \delta_{i0}\mathbf{I}_2)$$

$$\mathbf{M}_{kz} = \begin{pmatrix} 1 & 1 & 0.25 \\ k_{dzl0} & 0 & 0 \\ 0 & 1 & 0 \end{pmatrix}$$

$$\mathbf{I}_2 = \begin{pmatrix} 1 & 0 \\ 0 & 1 \end{pmatrix}$$

Thus, based on the above analysis and transformation, the structure of guidance control system considering disturbance is transformed in Fig. 8.

By the linear fractional transformation, the uncertainty is separated from the guidance system, and the standard form of robust control system is obtained, (8), shown at the bottom of this page.

The schematic diagram of the standard robust control system is presented in Fig. 9. M is the mathematical model of guidance system considering disturbance, K is the robust controller [13]–[17].

In order to design a robust guidance controller, the input of system $\omega = (\omega_1 \ \omega_2 \ \omega_3 \ \omega_4)^T = (y_{kdi} \ y_{kz1} \ y_{kz2} \ \omega_4)^T$ are specified, and the output of system $\mathbf{z} = (z_1 \ z_2 \ z_3 \ z_4)^T$ and its weight function W_1, W_2, W_3, W_4 are specified respectively. Where, ω_4 is the input noise and W_5 is the weight function.

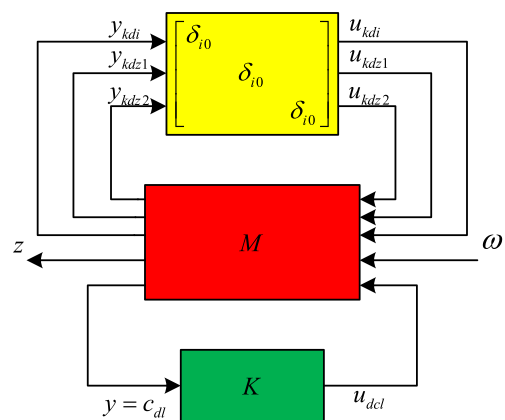


FIGURE 9. The schematic diagram of the standard robust control system.

According to the analysis of uncertainty in the guidance system, it is found that only if $W_4 \geq 0.5k_{dl0}$, $W_2 \geq k_{dz0}$ are set up, the change of static working current is less than $\pm 50\%$. In other words, $W_2 = k_{w2} \geq 0.5k_{dl0}$, $W_4 = k_{w4} \geq k_{dz0}$. Meanwhile, in order to avoid increasing the order of control system, W_3 is often set to be constant, namely, $W_3 = k_{w3}$. W_1 is the weight of system input, and is generally set to be a high-pass transfer function.

$$W_1 = k_{w1} \frac{s + 2\pi f_{w12}}{s + 2\pi f_{w11}}$$

W_5 is the weight of noise input, and generally set to be a low-pass transfer function.

$$W_5 = \frac{k_{w5}}{s + 2\pi f_{w5}}$$

The input is specified to be y , and the output is specified to be $u = u_{dcl}$. The state equation of the generalized guidance system is written as, (9), shown at the bottom of the next page.

The parameters of robust control system are indicated in the Table. 2, and submitted into the generalized state space

$$(\dot{c}_{dl} \quad \ddot{c}_{dl} \quad \dot{i}_{dl}) = F_l(\mathbf{M}, \Delta) \begin{pmatrix} c_{dl} \\ \dot{c}_{dl} \\ i_{dl} \\ u_{dcl} \end{pmatrix}$$

$$\mathbf{M} = \begin{pmatrix} 0 & 1 & 0 & 0 & 0 & 0 & 0 \\ \frac{1}{M_d}k_{dzl0} & 0 & -\frac{1}{M_d}k_{dil0} & 0 & -\frac{1}{M_d} & \frac{1}{M_d} & \frac{0.25}{M_d} \\ 0 & 0 & -\frac{R_d}{L_{dl0}} & \frac{1}{L_{dl0}} & 0 & 0 & 0 \\ 0 & 0 & 0.5k_{dil0} & 0 & 0 & 0 & 0 \\ 1 & 0 & 0 & 0 & 0 & 0 & 0 \\ 0 & 0 & 0 & 0 & 0 & 1 & 0 \end{pmatrix}$$

$$\Delta = \begin{pmatrix} \delta_{i0} & 0 & 0 \\ 0 & \delta_{i0} & 0 \\ 0 & 0 & \delta_{i0} \end{pmatrix} \quad (8)$$

TABLE 2. Parameters of robust control system.

Symbol	Quantity	Unit
k_{w1}	1×10^5	
k_{w2}	5×10^5	
k_{w3}	1×10^{-2}	
k_{w4}	126	
k_{w5}	4.0×10^{-7}	
f_{w5}	20	Hz
f_{w11}	20	Hz
f_{w12}	5	Hz
i_{dl0}	20	A

equation of the guidance system (9). The robust control toolbox of MATLAB for H_∞ control theory is adopted, and the robust controller is designed.

$$\dot{\mathbf{x}}_c = \begin{pmatrix} -90967 & -783 & 3265 & 27035 & -212310 \\ 0 & -46 & 7 & 58 & -477 \\ 0 & -16 & -126 & -3 & 31 \\ 0 & -129 & -5 & -165 & 347 \\ 0 & 3387 & 382 & 3237 & -26565 \end{pmatrix} \mathbf{x}_c + \begin{pmatrix} 0 \\ -2037800 \\ -1454900 \\ -11498000 \\ 307310000 \end{pmatrix} y + \begin{pmatrix} 12604 & 108 & -453 & -3747 & 29423 \end{pmatrix} \mathbf{x}_c \quad (10)$$

In order to examine the performance of the designed robust controller in the single electromagnet model, the left

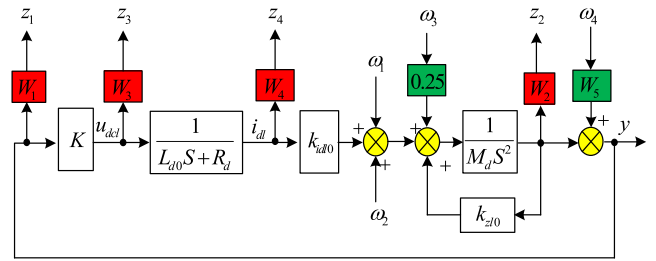


FIGURE 10. The control structure of the robust guidance system.

guidance electromagnet is impacted on a step interference force of 2000 N. The responses of guidance system are shown in Fig.11(a), Fig.11(b)and Fig.11(c) respectively.

When the initial static working current of left guidance electromagnet is set as 10 A, the maximum gap error fluctuation is 2.3 mm; When the initial static working current is set as 20 A, the maximum gap error fluctuation becomes 1.8 mm. When the initial static working current is set as 30 A, the maximum gap error fluctuation becomes 1.5 mm. Compared with the performance of the previous state feedback controller, the simulation and verification demonstrate that the robust controller of guidance system in single electromagnet model has better robustness.

In order to achieve an overall evaluation of the designed robust controller in the single electromagnet model, the left guidance gap signal is assumed to be subjected to 3mm step disturbance. When the initial static working currents are set as 10 A, 20 A and 30 A, the responses of guidance system are shown in Fig. 12(a), Fig. 12(b) and Fig. 12(c) respectively.

When the static working current of robust controller in the single electromagnet model changes three times, the gap error change is only 1.5 times. While the static working current of the general state feedback controller changes two times, the gap error change is 1.8 times. Obviously, the robust controller has better robustness. On the other hand, when the

$$\begin{pmatrix} \dot{\mathbf{x}} \\ \mathbf{z} \\ \mathbf{y} \end{pmatrix} = \begin{pmatrix} \mathbf{A} & \mathbf{B}_1 & \mathbf{B}_2 \\ \mathbf{C}_1 & \mathbf{D}_{11} & \mathbf{D}_{12} \\ \mathbf{C}_2 & \mathbf{D}_{21} & \mathbf{D}_{22} \end{pmatrix} \begin{pmatrix} \mathbf{x} \\ \omega \\ u \end{pmatrix} = \begin{pmatrix} 0 & 1 & 0 & 0 & 0 & 0 & 0 & 0 & 0 & 0 & 0 \\ \frac{1}{M_d}k_{dzl0} & 0 & -\frac{1}{M_d}k_{dil0} & 0 & 0 & -\frac{1}{M_d} & \frac{1}{M_d} & \frac{0.25}{M_d} & 0 & 0 & 0 \\ 0 & 0 & -\frac{R_d}{L_{dl0}} & 0 & 0 & 0 & 0 & 0 & 0 & 0 & \frac{1}{L_{dl0}} \\ 0 & 0 & 0 & -2\pi f_{w5} & 0 & 0 & 0 & 0 & 1 & 0 & 0 \\ 1 & 0 & 0 & -k_{w5} & -2\pi f_{w11} & 0 & 0 & 0 & 0 & 0 & 0 \\ k_{w1} & 0 & 0 & -k_{w1}k_{w5} & -2\pi k_{w1}(f_{w11} - f_{w12}) & 0 & 0 & 0 & 0 & 0 & 0 \\ k_{w2} & 0 & 0 & 0 & 0 & 0 & 0 & 0 & 0 & 0 & 0 \\ 0 & 0 & k_{w4} & 0 & 0 & 0 & 0 & 0 & 0 & 0 & 0 \\ 0 & 0 & 0 & 0 & 0 & 0 & 0 & 0 & 0 & 0 & 1 \\ 1 & 0 & 0 & 0 & 0 & 0 & 0 & 0 & -k_{w5} & 0 & 0 \end{pmatrix} \begin{pmatrix} \mathbf{x} \\ \omega \\ u \end{pmatrix} \quad (9)$$

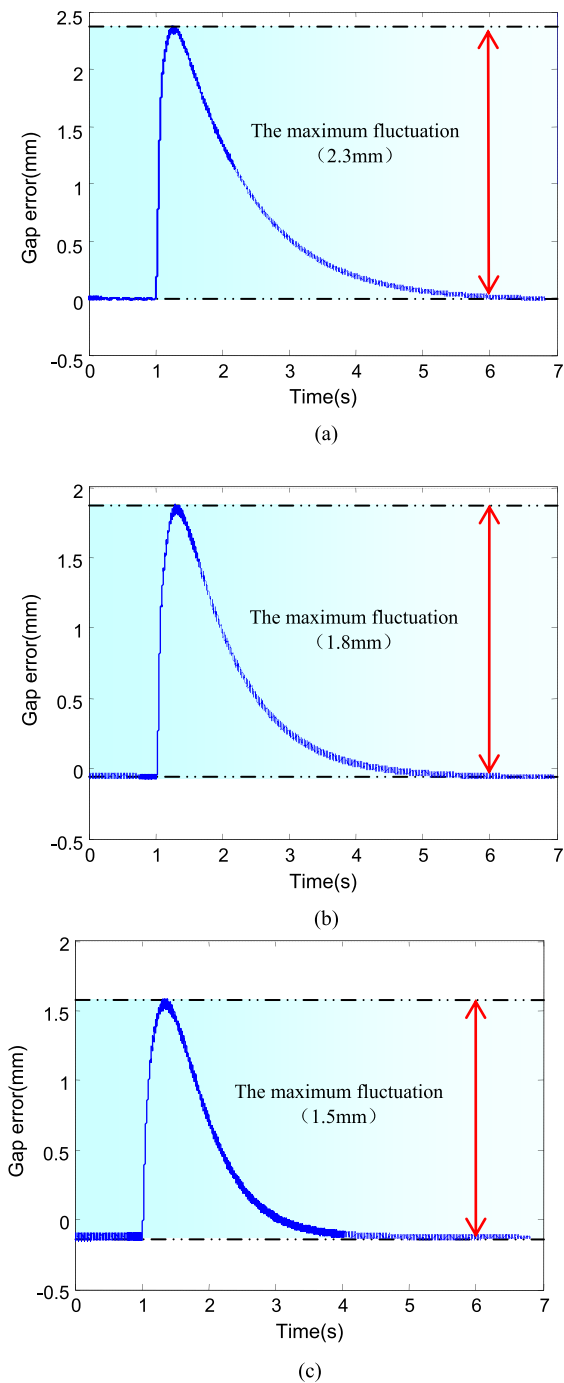


FIGURE 11. The response of designed robust guidance controller with different Initial static current in single electromagnet model. (a) Static working current is 10 A. (b) Static working current is 20 A. (c) Static working current is 30 A.

guidance gap signal is subjected to 3mm step disturbance, the response of the guidance system which using robust controller is very close, with only a slight difference in amplitude.

The simulation shows the robust controller has the ability to guarantee the stability of the system under different working currents, and obtain similar performance to improve the guidance system robustness.

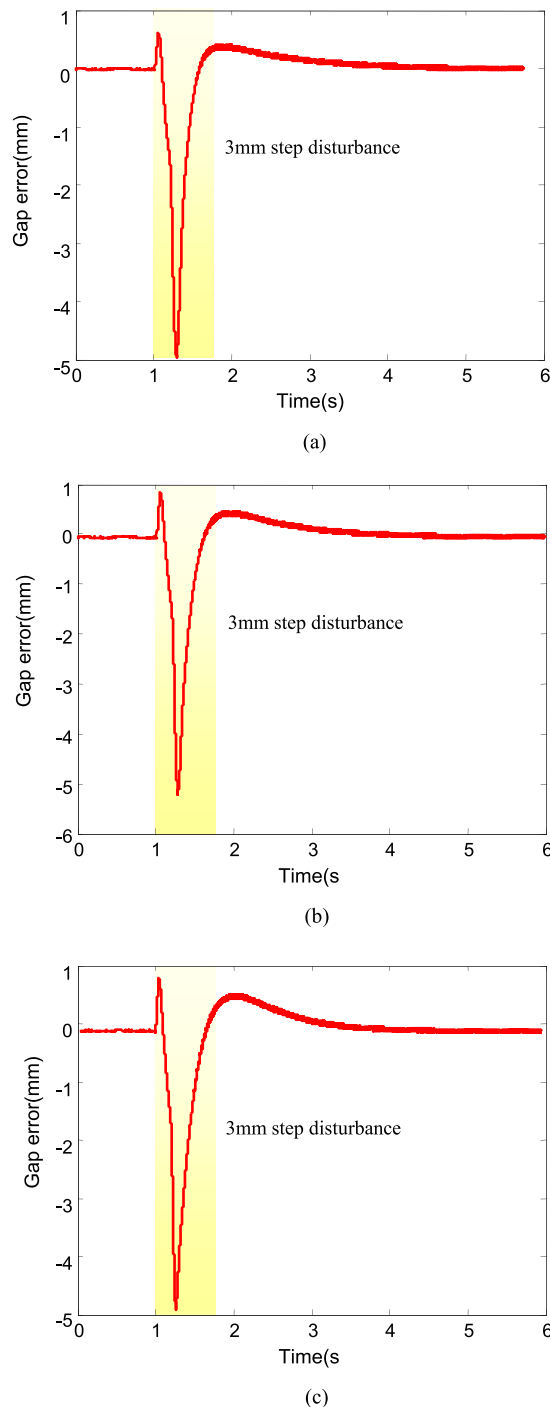


FIGURE 12. The response of robust guidance system by 3mm step disturbance. (a) Static working current is 10 A. (b) Static working current is 20 A. (c) Static working current is 30 A.

V. EXPERIMENT AND VERIFICATION

In order to verify the rationality of the above analysis and have an overall evaluation of the robust controller, the test platform of the dual suspension frames is built. The dual suspension frames are the minimum function unit of levitation and guidance for high-speed maglev train, which includes the basic joint-structure and pendulum structure of the entire

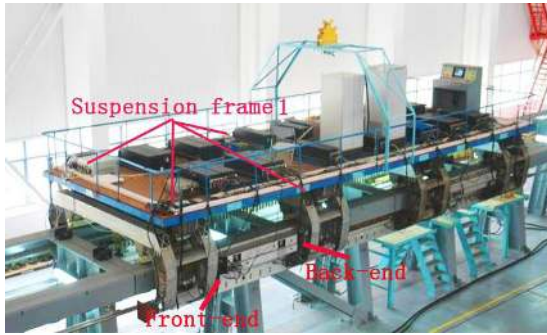


FIGURE 13. The photograph of dual suspension frames.

vehicle system. A complete high-speed maglev train is composed of five such suspension frames. The weights on the dual suspension frames are used to simulate the weight of the carriage and the load. The platform is able to accurately examine the working conditions of suspension and guidance system.

The guidance system consists of guidance controllers, sensors and guidance electromagnets. Guidance controllers adjust the left and right guiding current based on the gaps between the electromagnets and guide way, to ensure that the gap between the left and right sides is equal approximately.

When the dual suspension frames is suspended in the straight line and the guidance system is opened, the guidance gap and current of front-end and back-end in suspension frame 1 are measured in Fig.14(a), Fig.14(b), Fig.14(c) and Fig.14(d) respectively.

As shown in Fig. 14, when the dual suspension frames is suspended and the guidance system is closed, the guidance electromagnets oscillate slightly along the lateral direction of the guide way. The guidance currents of front-end and back-end in suspension frame 1 are zero, and the guidance gaps of front-end and back-end in suspension frame 1 fluctuate up and down in 11mm. After the guidance system is opened, the guidance electromagnets quickly enter into a stable state. The steady guidance gaps of front-end and back-end on the suspension frame 1 are 11.5 mm and 11.3 mm respectively. The steady guidance currents of front-end and back-end on the suspension frame 1 are almost 5 A.

The experiment results show that the guidance system is working in double electromagnet model in the straight line. The guidance gap is kept in the setting gap under the action of the designed guidance controller, and the dual suspension frames is located directly above the guide way centerline and doesn't move left or right. This is our expectation about guidance system.

In order to examine the performance of guidance system through the bend, the dual suspension frames is suspended and passes through the bend with 400 meters curvature-radius at a speed of 25 km/h. In the process, the guidance system is opened and the guidance gaps and currents are measured in Fig.15(a), Fig.15(b), Fig.15(c) and Fig.15(d) respectively.

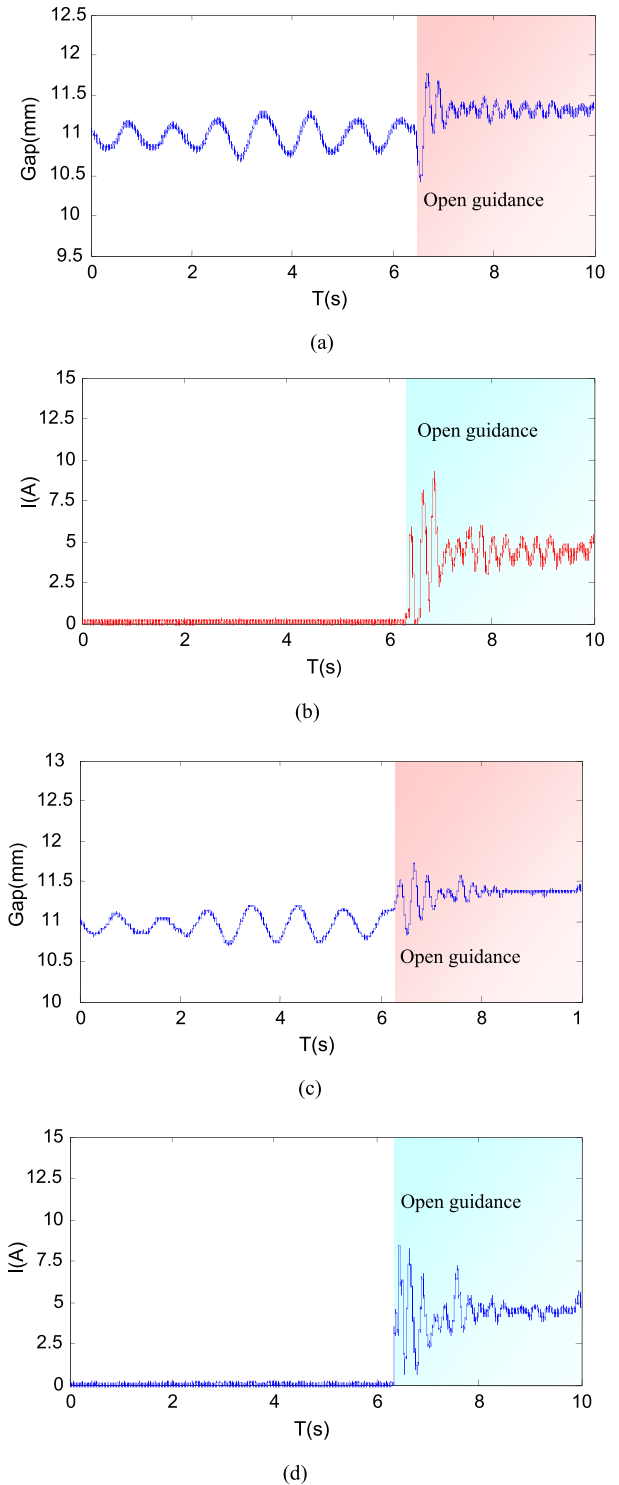


FIGURE 14. The guidance gap and current measured on the suspension frame 1. (a) The guidance gap of front-end. (b) The guidance current of front-end. (c) The guidance gap of back-end. (d) The guidance current of back-end.

As shown in Fig. 15, when the dual suspension frames is suspended and passes through the bend at speed of 25 km/h, the guidance current of outside electromagnet in suspension frame 1 increases 25 A rapidly in order to supply adequate

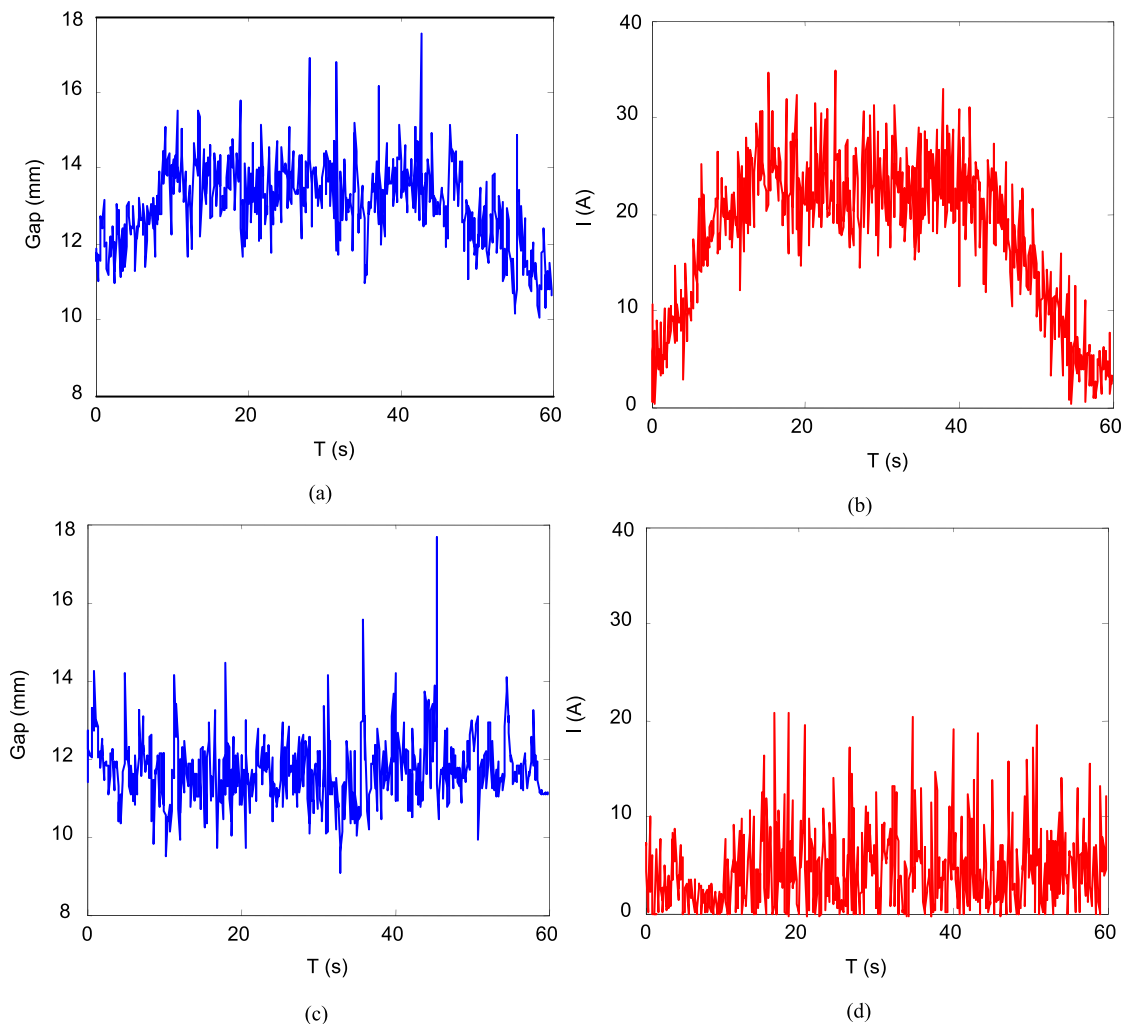


FIGURE 15. The performance of the suspension frame 1 when passing through the bend at a speed of 25 km/h. (a) The outside guidance gap. (b) The outside guidance current. (c) The inside guidance gap. (d) The inside guidance current.

guidance force. The guidance gap of outside electromagnet has a little increase. On the other side, the guidance current of inside electromagnet fluctuates between 0 and 5 A, and the guidance gap has a little decrease.

When the dual suspension frames is suspended and passes through the bend with 400 meters curvature-radius at a speed of 25 km/h, the dual suspension frames needs guidance system to provide guidance force, and then the guidance system enters the single electromagnet model. The guidance gap keeps fluctuating near the setting gap under the action of the designed robust guidance controller, and the dual suspension frames do not deviate greatly from the lateral direction. The entire dual suspension frames runs smoothly along the line through the bend.

The results demonstrate that the designed guidance robust controller is able to supply stable guidance ability on different conditions to ensure that the dual suspension frames passes through the bend smoothly.

VI. DISCUSSION

In this paper, the emphasis is on the design and implementation of the guidance control system. Meanwhile, the test platform of the dual suspension frames is established and the basic functions of the guidance system are verified by using the dual suspension frames. When the dual suspension frames is suspended in the straight line and the guidance system is opened, the guidance gap is kept in the setting gap, and the dual suspension frames is located directly above the guide way centerline. When the dual suspension frames is suspended and passes through the bend with 400 meters curvature-radius at a speed of 25 km/h, the guidance gap keeps fluctuating near the setting gap, and the dual suspension frames do not deviate greatly from the lateral direction. However, the required guidance force is different when the high-speed maglev train passes through the bend with different curvature-radius and different speeds. Therefore, the working characteristics of the guidance system in the

different curvature-radius and speed conditions need to be further analysis, calculation and verification. This will become a study emphasis in further research.

VII. CONCLUSION

The study demonstrates that the designed guidance robust controller is able to supply stable guidance ability on different conditions. It is of vital importance that the high-speed maglev train can pass through bend smoothly and resist the crosswind. The mathematical model of guidance system is established, and the robust guidance controller is designed to solve the guidance problem successfully, which ensure the safety and improve the reliability of high-speed maglev train greatly.

REFERENCES

- [1] M. Janic, "Multicriteria evaluation of high-speed rail, transrapid Maglev and air passenger transport in Europe," *Transp. Planning Technol.*, vol. 26, no. 6, pp. 491–512, 2016.
- [2] H.-W. Lee, K.-C. Kim, and J. Lee, "Review of Maglev train technologies," *IEEE Trans. Magn.*, vol. 42, no. 7, pp. 1917–1925, Jul. 2006.
- [3] H. M. Gutierrez and H. Luijten, "5-DOF real-time control of active electrodynamic MAGLEV," *IEEE Trans. Ind. Electron.*, vol. 65, no. 9, pp. 7468–7476, Sep. 2018.
- [4] L. Yan, "Development and application of the Maglev transportation system," *IEEE Trans. Appl. Supercond.*, vol. 18, no. 2, pp. 92–99, Jun. 2008.
- [5] G. Lin, "Application and development of Maglev transportation in China," Maglev, Berlin, Germany, Tech. Rep., 2016.
- [6] Y. Lee, J.-W. Park, C.-W. Ha, J. Lim, and C.-H. Kim, "Design and control characteristics of guidance system for passive Maglev transport system," in *Proc. IEEE Conf. Electromagn. Field Comput.*, Nov. 2016, p. 1.
- [7] M. Kim, J.-H. Jeong, J. Lim, M.-C. Won, and C.-H. Kim, "Design and control of levitation and guidance systems for a semi-high-speed maglev train," *J. Electr. Eng. Technol.*, vol. 12, no. 1, pp. 117–125, Jan. 2017.
- [8] D.-J. Min, S.-D. Kwon, J.-W. Kwark, and M.-Y. Kim, "Gust wind effects on stability and ride quality of actively controlled Maglev guideway systems," *Shock Vib.*, vol. 2017, Apr. 2017, Art. no. 9716080.
- [9] J. Shi, W.-S. Fang, Y.-J. Wang, and Y. Zhao, "Measurements and analysis of track irregularities on high speed Maglev lines," *J. Zhejiang Univ. Sci. A.*, vol. 15, no. 6, pp. 385–394, Jun. 2014.
- [10] J.-H. Jeong, C.-W. Ha, J. Lim, and J.-Y. Choi, "Analysis and control of electromagnetic coupling effect of levitation and guidance systems for semi-high-speed maglev train considering current direction," *IEEE Trans. Magn.*, vol. 53, no. 6, Jun. 2017, Art. no. 8300204.
- [11] C. H. Kim, C. W. Ha, J. Lim, H. S. Han, and K. J. Kim, "Yaw motion control of electromagnetic guidance system for high-speed Maglev vehicles," *J. Electr. Eng. Technol.*, vol. 11, no. 5, pp. 1299–1304, 2016.
- [12] J. Xu, C. Chen, D. Gao, S. Luo, and Q. Qian, "Nonlinear dynamic analysis on Maglev train system with flexible guideway and double time-delay feedback control," *J. Vibroengineering*, vol. 19, no. 8, pp. 6346–6362, 2017.
- [13] J. Yang, A. Zolotas, W.-H. Chen, K. Michail, and S. Li, "Robust control of nonlinear MAGLEV suspension system with mismatched uncertainties via DOBC approach," *ISA Trans.*, vol. 50, no. 3, pp. 389–396, 2011.
- [14] E. Kong, J.-S. Song, B.-B. Kang, and S. Na, "Dynamic response and robust control of coupled Maglev vehicle and guideway system," *J. Sound Vib.*, vol. 330, no. 25, pp. 6237–6253, 2011.
- [15] X. Hu, S. Li, H. Peng, and F. Sun, "Robustness analysis of state-of-charge estimation methods for two types of Li-IoN batteries," *J. Power Sour.*, vol. 217, pp. 209–219, Nov. 2012.
- [16] F. Gao, X. Hu, S. E. Li, K. Li, and Q. Sun, "Distributed adaptive sliding mode control of vehicular platoon with uncertain interaction topology," *IEEE Trans. Ind. Electron.*, vol. 65, no. 8, pp. 6352–6361, Aug. 2018.
- [17] C. Zou, X. Hu, S. Dey, L. Zhang, and X. Tang, "Nonlinear fractional-order estimator with guaranteed robustness and stability for lithium-ion batteries," *IEEE Trans. Ind. Electron.*, vol. 65, no. 7, pp. 5951–5961, Jul. 2018.



MINGDA ZHAI received the M.S. degree in control science and engineering from the National University of Defense Technology, Changsha, China, in 2015, where he is currently pursuing the Ph.D. degree in control science and engineering. His current research interests include magnetic levitation control, fault diagnosis, tolerant control for maglev trains, and new maglev technology.



AMING HAO received the Ph.D. degree in control science and engineering from the National University of Defense Technology, Changsha, China, in 2008. He is currently a Lecturer with the National University of Defense Technology. His current research interests include magnetic levitation control, fault diagnosis, tolerant control for maglev trains, and new maglev technology.



XIAOLONG LI received the Ph.D. degree in control science and engineering from the National University of Defense Technology, Changsha, China, in 2009, where he is currently an Associate Research Fellow. His current research interests include magnetic levitation control and new maglev technology.



ZHIQIANG LONG received the B.S. degree in automation from the Huazhong University of Science and Technology, Wuhan, China, in 1988, the M.S. degree in flight mechanics from the Harbin Institute of Technology, Harbin, China, in 1991, and the Ph.D. degree in control science and engineering from the National University of Defense Technology, Changsha, China, in 2010.

He is currently a Professor with the National University of Defense Technology, where he is also the Head Research Engineer of the Engineering Research Center of Maglev Technology. His current research interests include magnetic levitation control, fault diagnosis, tolerant control for maglev trains, and new maglev technology.

...